Electronic Supporting Information for

Adhesion Strength of Aluminum Surfaces Coated with Silane Coupling Protective Layers via Acid-Base Interactions

Kumpei Kobori[1], *Shuji Ogata*[2*], *Shintaro Yamamoto*[3], *Yusuke Takahashi*[3], *Takayuki Miyamae*[1,4,5*]

[1]Graduate School of Science and Engineering, Chiba University, 1-33 Yayoi-cho, Inage-ku, Chiba 263-8522, Japan.

[2]Nagoya Institute of Technology, Gokiso-cho, Showa-ku, Nagoya 466-8555, Japan.

[3] Materials Research Laboratory, Technical Development Group, Kobe Steel Ltd. 5-5 Takatsukadai 1-chome, Nishi-ku, Kobe 651-2271, Japan.

[4]Molecular Chirality Research Center, Chiba University, 1-33 Yayoi-cho, Inage-ku, Chiba-shi 263-8522, Japan

[5]Soft Molecular Activation Research Center, Chiba University, 1-33 Yayoi-cho, Inage-ku, Chiba, Chiba 263-8522, Japan

[*]Authors to whom correspondence should be addressed: ogata@nitech.ac.jp and t-miyamae@chiba-u.jp

S.1 Simulation system to analyze acidity: BTSE connected to HO-terminated γ-alumina

When gradually exposed to oxygen in the air, aluminum metal develops a surface oxide layer with a depth ranging from 5 to 40 Å.[1-3] The internal structure of this surface oxide is not well understood experimentally. Theoretical calculations of free energy, which account for elastic deformation due to lattice mismatch at the Al-oxide interface, suggested that the surface oxide on Al (111) adopts an amorphous structure at depths of 5–10 Å and γ-alumina at greater depths under ordinary conditions.[2] The γ-alumina transforms to α-alumina (the most stable phase of alumina) at high temperatures (~ 900 K).[3] With this in mind, we prepared a γ-alumina slab as a substrate to which a silane compound connects for the present simulations as follows.

The atomic structure of γ-alumina is usually described as a defective spinel.[4] We constructed the spinel (i.e., $MgAl_2O_4$) cubic unit cell with a volume of $(7.929Å)^3$, consisting of 56 atoms. In this structure, 32 O atoms formed the face-centered cubic (FCC) lattice, while 8 Mg (16 Al) atoms occupied the tetrahedral (octahedral) sites of the FCC lattice. All Mg atoms were replaced by Al to make a unit cell with a stoichiometry ratio of Al:O = 3:4. The γ-alumina slab was created by assembling $3 \times 2 \times 1$ unitcells and then randomly removing Al atoms from the octahedral sites to achieve a stoichiometry ratio of Al:O = 2:3. Side lengths of the γ-alumina slab were $(L_x, L_z) = (23.787, 15.858)$ Å under periodic boundary conditions (PBCs) with a y-depth of 7.929 Å.

Proper termination of the γ-alumina surface is crucial. Previous experiments indicated that the point of zero charge (PZC) for γ-alumina is 9.2, which was anticipated to result from three pK_a relating to three types of surface sites:[5] pK_a12.5 for the adsorption equilibration $(Al_{oh})_2 - OH' \rightleftharpoons (Al_{oh})_2 - O$, 9.6 for $Al_{oh} - (OH)'H' \rightleftharpoons Al_{oh} - (OH)'$, and 6.7 for $Al_{th} - (OH)'H' \rightleftharpoons Al_{th} - (OH)'$, where Al_{oh} and Al_{th} represent octahedral and tetrahedral Al, respectively, and H' and $(OH)'$ are adsorbed from the surrounding water. Since no Al_{th} is present

on the top surface of present γ-alumina model, we anticipated the presence of $(Al_{oh})_2 - OH'$ and $Al_{oh} - (OH)'H'$ under pH 7, meaning the number of H' exceeds that of $(OH)'$. Considering this, we initially placed 24 OH and 36 H on the top surface of γ-alumina. Through a density-functional theory (DFT)-based molecular dynamics (MD) simulation for thermalization conducted for 5 ps at 298 K, we removed 15 H_2O and 2 H_2 that formed and desorbed from the surface. This process resulted in 12 surface-sites of Al_2-OH, 5 of Al-OHH, and 4 of Al-OH to mimic a HO-terminated γ-alumina, as shown in **Figs. 2 (a)** and **(b)** in the text.

S.2 Settings of DFT-MD simulation

We applied the DFT for electrons to calculate the forces on atoms required for MD simulation and for configuration sampling.[6] The adiabatic approximation was adopted for electrons, that is, electronic structure is calculated in the ground state for a given set of nuclear positions at each timestep. Since statistical configuration average is not affected by the mass change of H in the adiabatic approximation, deuterium mass was set for H to allow the use of a timestep of 1.4 fs.[6-10] The Troullier and Martins (TM)-type norm-conserving pseudopotentials[11] were used for the valence electrons. The Perdew-Burke-Ernzerhof-type (PBE) generalized gradient approximation (GGA) exchange-correlation functional[12] was adopted in the real-space-grid type DFT code (DC-RGDFT).[6] The choice of PBE-GGA is because it has been successfully used for calculations of protonation degrees for both inorganic and organic systems in water as well as microscopic structure of liquid water.[7-10,13] We set the grid size $h = 0.40a_B$ with Bohr radius $a_B = 0.5292$ Å to use DC-RGDFT, which corresponds to the cutoff energy $\left(\frac{\pi}{h}\right)^2 Ry = 840\ eV$ ($1\ Ry = 13.61\ eV$) in the plane-wave implementation of DFT. A finer grid of $h/3$ was also set around each C, N, and O nucleus for the pseudopotentials.[6]

References

1 J. M. McHale, A. Auroux, A. J. Perrotta, A. Navrotsky, *Science,* 1997, **227**, 788−791.

2 L. P. H. Jeurgens, W. G. Sloof, F. D. Tichelaar, E. J. Mittmeijer, *Phys. Rev. B*, 2000, **62**, 4707−4719.

3 M. A. Trunov, M. Schoenitz, E. L. Dreizin, *Propel. Explos. Pyrotech*., 2005, **30**, 36−43.

4 F. H. Streitz, J. W. Mintmire, *Phys. Rev. B,* 1999, **60**, 773−777.

5 C. Cristian, J. Jagiello, J. A. Schwarz, *Langmuir*, 1993, **9**, 1754−1765.

6 N. Ohba, S. Ogata, T. Kouno, T. Tamura, R. Kobayashi, *Comput. Phys. Commun*., 2012, **183**, 1664–1673.

7 S. Ogata, M. Uranagase, Y. Takahashi, T. Kishi, *J. Phys. Chem. B*, 2021, **125**, 8989−8996.

8 S. Ogata, M. Uranagase, *J. Phys. Chem. B*, 2023, **127**, 2629−2638; *ibid*. 2023, **127**, 6833–6834.

9 S. Ogata, M. Uranagase, Y. Takahashi, T. Kishi, *MRS Commun*., 2022, **12**, 315−321.

10 P. N. A. M. Ariff, D. M. Sedgwick, K. Iwasawa, T. Kiyono, Y. Sumii, R. Ikuta, M. Uranagase, H. Kawahara, S. Fustero, S. Ogata, N. Shibata, *J. Am. Chem. Soc*., 2024, **146**, 26435−26441.

11 N. Troullier, J. L. Martins, *Phys. Rev. B,* 1991, **43**, 1993–2006.

12 J. P. Perdew, K. Burke, M. Ernzerhof, *Phys. Rev. Lett*., 1996, **77**, 3865–3868; Erratum. *Phys. Rev. Lett.,* 1997, **78**, 1396.

13 M. J. Gillan, D. Alfè, A. Michaelides, *J. Chem. Phys*., 2016, **144**, 130901.

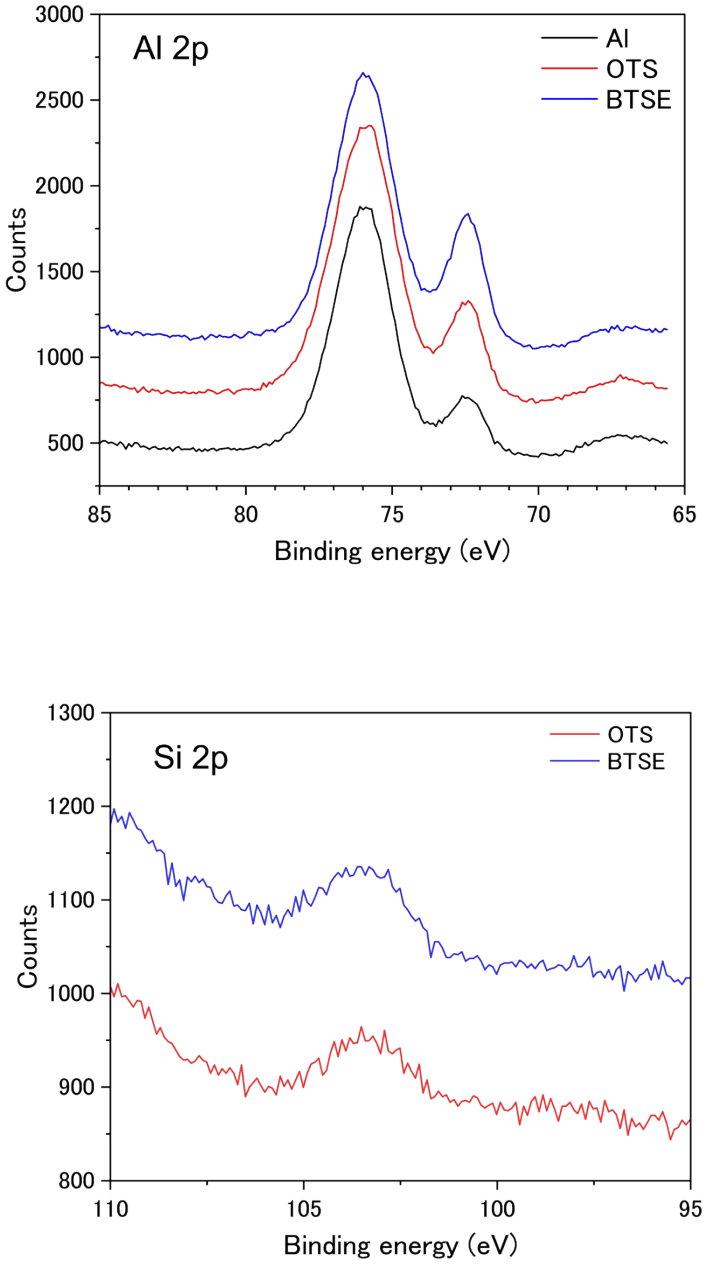

Figure S1. XPS spectra of the Al2p region and Si2p region for the chemically polished Al substrate (black), OTS-treated (red), and BTSE-treated (blue) samples. XPS measurements were performed using JPS-9030 manufactured by JEOL Ltd. The X-ray source used in XPS was AlKα.

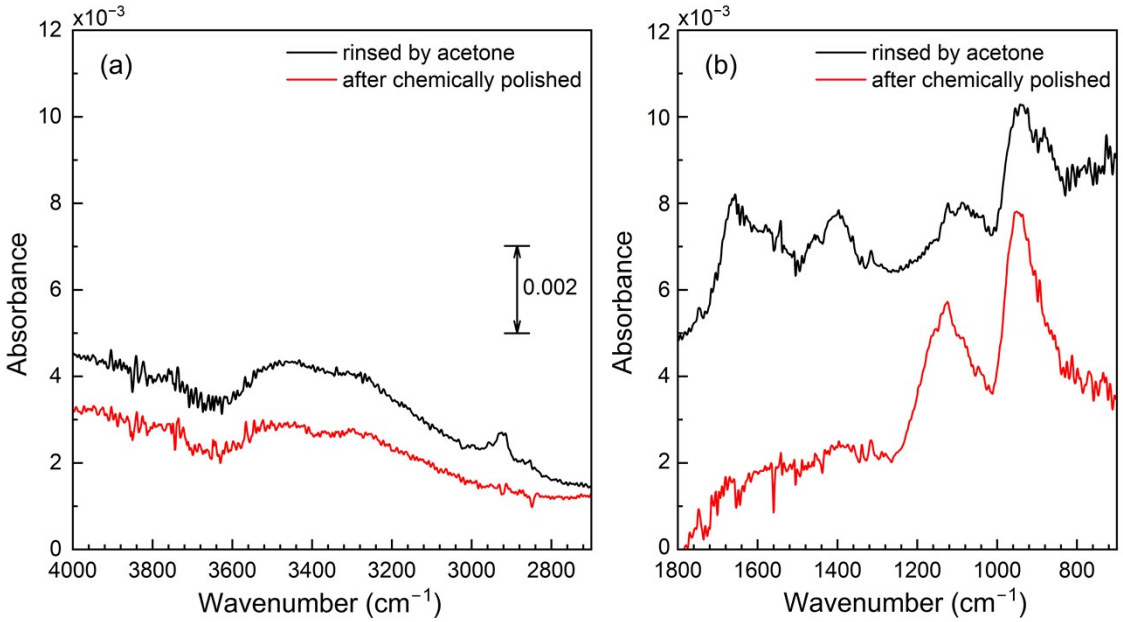

Figure S2. ATR-IR spectra of acetone-cleaned Al substrate (black line) and chemically polished Al substrate (red line). (a) 4000–2700 cm^{-1} and (b) 1800–700 cm^{-1}. ATR-IR measurements were performed using a Fourier transform infrared spectrometer (FT-IR-6600) manufactured by JASCO Co. with 128 accumulation cycles and a resolution of 4 cm^{-1}. A diamond prism was used for ATR measurements

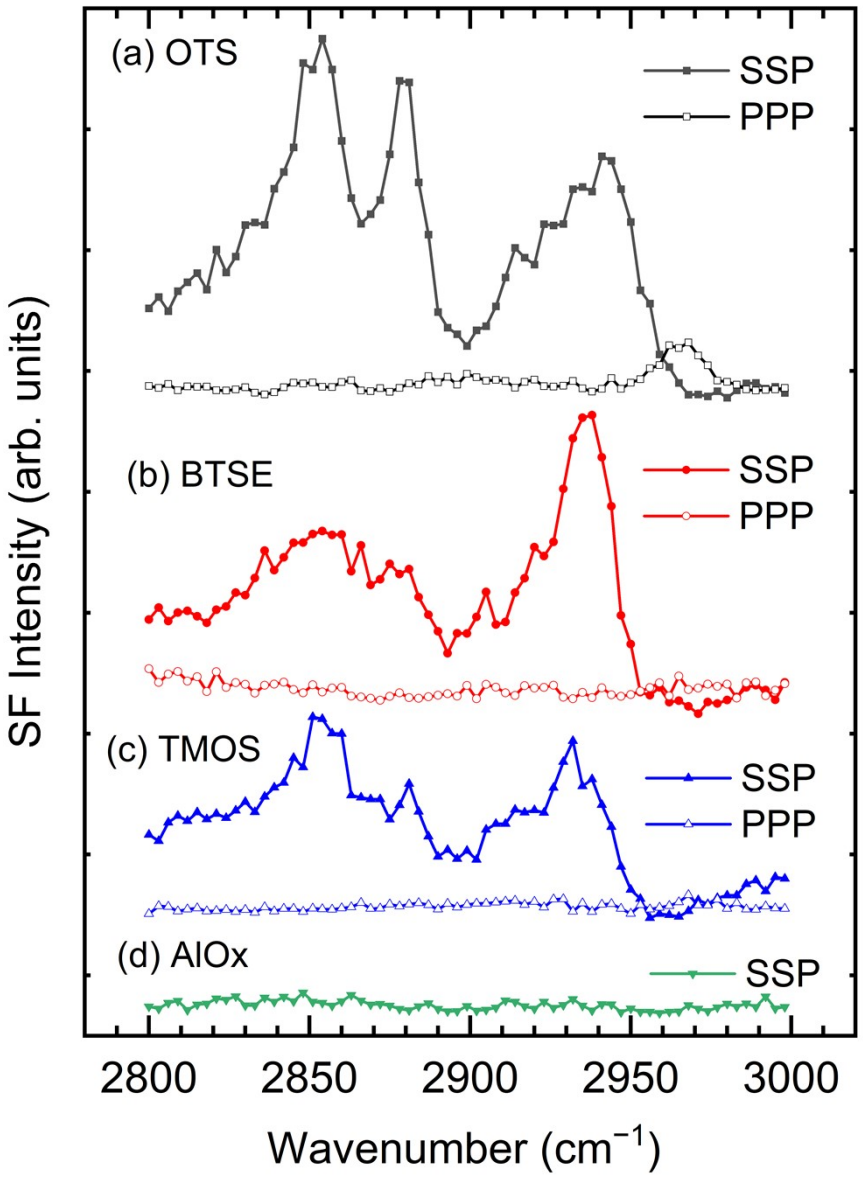

Figure S3. SSP and PPP polarized SFG spectra of (a) OTS adsorbed on AlO_x substrates, (b) (b) BTSE adsorbed on AlO_x substrates, (c) TMOS adsorbed on AlO_x substrates, and (d) SSP polarized SFG spectrum of AlOx-coated CaF_2 surface. The deposition conditions of silane agents are were compared under identical conditions. Spectra are offset for clarity

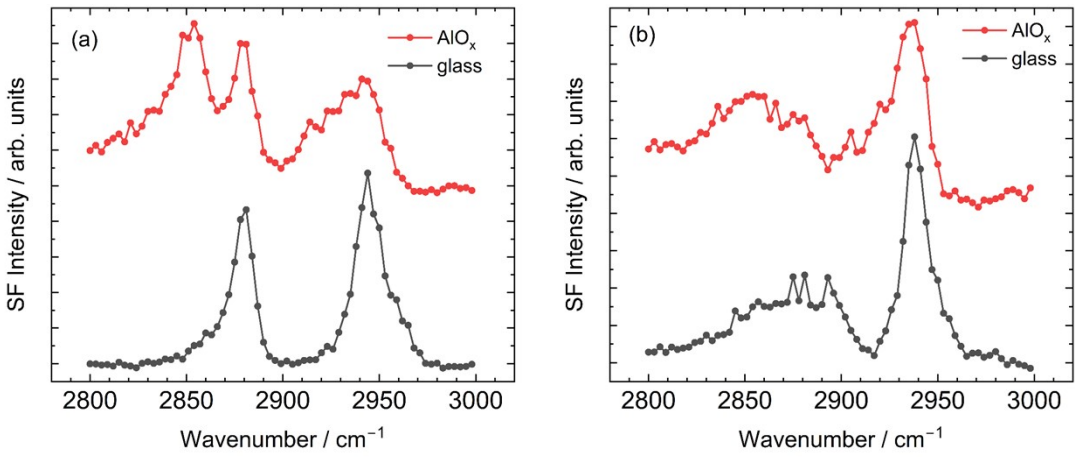

Figure S4. SSP polarized SFG spectra of (a) OTS adsorbed on glass and AlO_x substrates, and (b) BTSE adsorbed on glass and AlO_x substrates. The deposition conditions were compared under identical conditions.

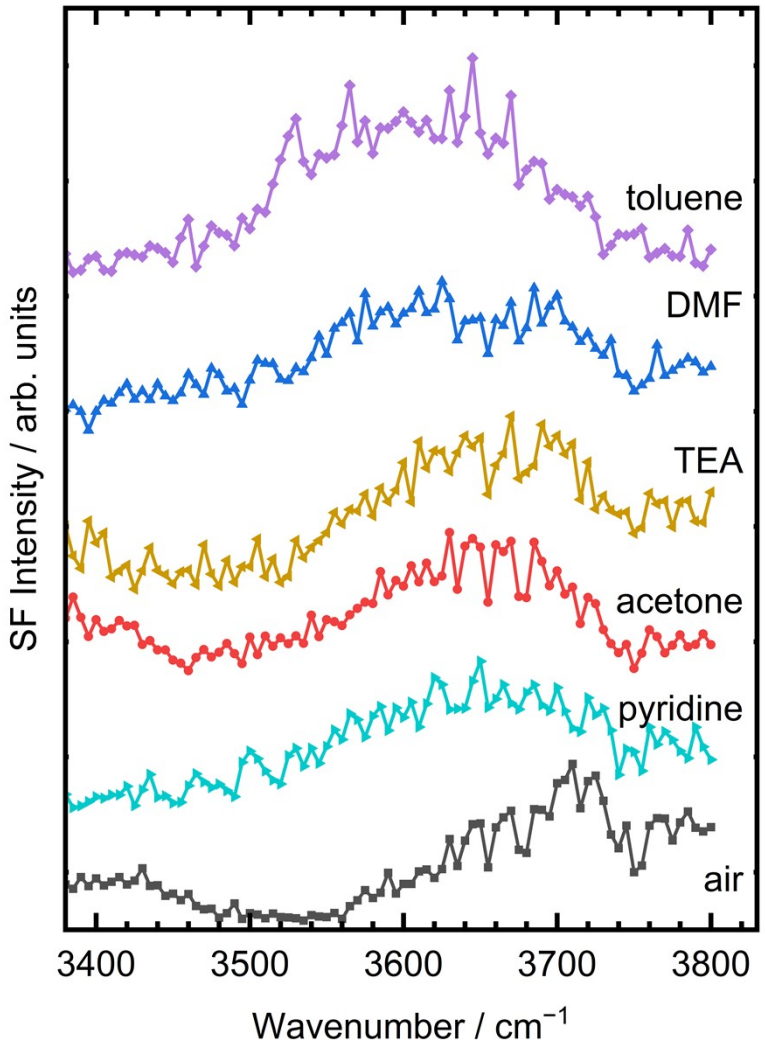

Figure S5. SSP polarized SFG spectra collected for five different liquids in contact with AlO_x-coated CaF_2 surfaces in the hydroxyl stretching region. The spectra are offset for clarity.

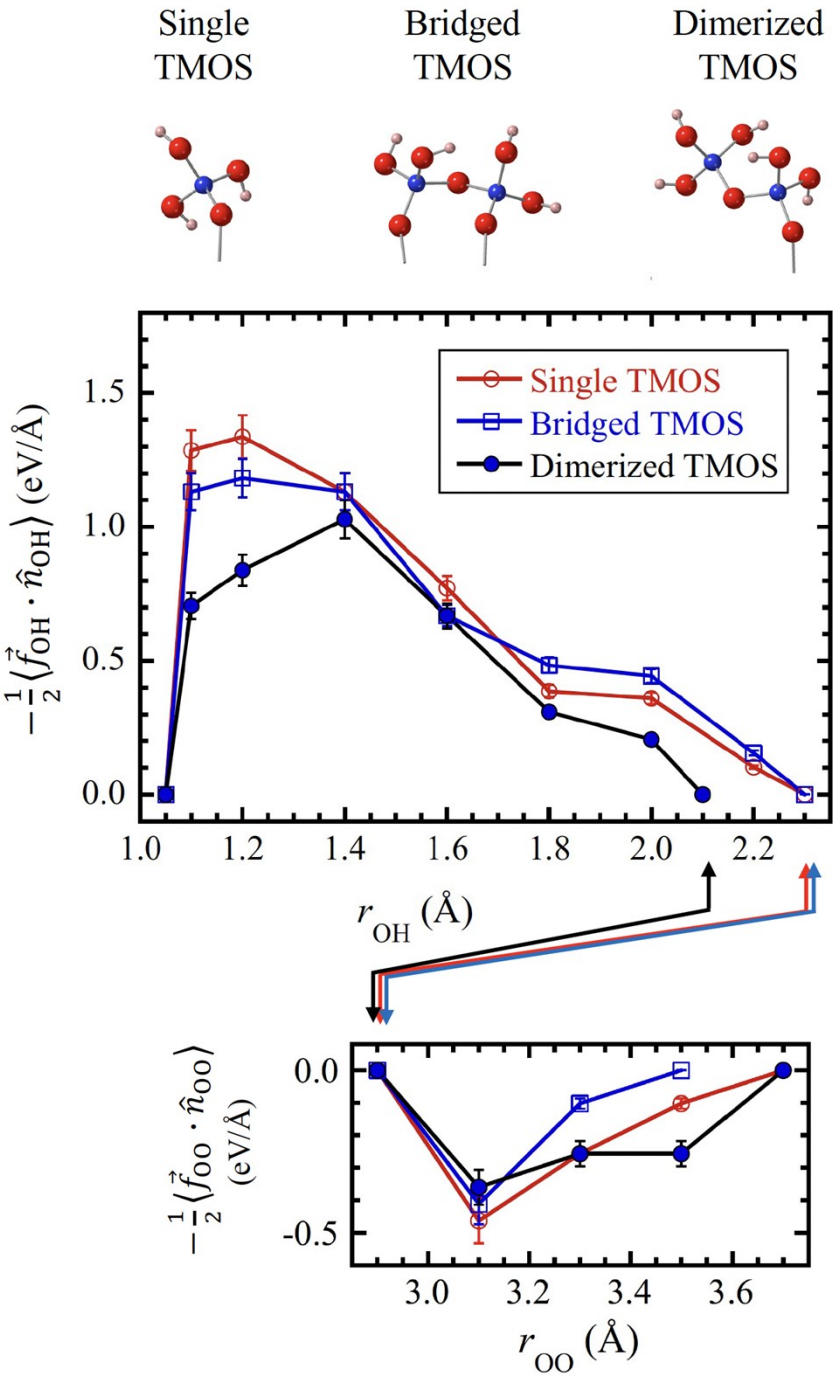

Figure S6. (top) Single, bridged, and dimerized forms of TMOS connected to HO-terminated γ-alumina. (Middle) The DFT-MD sampling result of $\langle \vec{f}_{OH} \cdot \hat{n}_{OH} \rangle$ at each r_{OH} for subprocess-(i) in the H^+-shift method. (Bottom) Same as (Middle), but of $\langle \vec{f}_{OO} \cdot \hat{n}_{OO} \rangle$ at each r_{OO} for subprocess-(ii).

Table S1. Fitting summary table for SFG spectra in Figure 6.

OTS	Peak 1			Peak 2		
Solvent	A_q	ω_q (cm^{-1})	Γ_q (cm^{-1})	A_q	ω_q (cm^{-1})	Γ_q (cm^{-1})
Pyridine	0.57	3593	108.7	0.21	3647	107.9
TEA	0.60	3592	97.9	0.60	3647	115.9
DMF	0.94	3589	131.6	0.47	3647	104.5
acetone	1.59	3604	166.3	0.43	3647	110.0
air	1.55	3647	117.5		—	
BTSE	Peak 1			Peak 2		
solvent	A_q	ω_q (cm^{-1})	Γ_q (cm^{-1})	A_q	ω_q (cm^{-1})	Γ_q (cm^{-1})
Pyridine	1.25	3590	133.0	0.79	3665	143.0
TEA	1.07	3590	121.9	0.51	3655	100.8
DMF	0.87	3589	120.5	1.01	3665	133.3
acetone	1.10	3601	123.4	0.98	3665	146.4
air	2.78	3655	131.9		—	
TMOS	Peak1			Peak2		
solvent	A_q	ω_q (cm^{-1})	Γ_q (cm^{-1})	A_q	ω_q (cm^{-1})	Γ_q (cm^{-1})
Pyridine	0.48	3597	161.0	0.45	3665	120.0
TEA	0.82	3593	115.0	0.05	3665	122.2
DMF	0.67	3598	119.4	0.42	3665	131.0
acetone	1.41	3604	140.0	0.10	3665	120.0
air	1.76	3665	136.8		—	

Table S2. Fitting summary table for SFG spectra collected for 10 wt% dicyandiamide DMF solution in contact with TMOS-treated, BTSE-treated, and OTS-treated AlO_x surfaces shown in Figure 8.

	Peak 0			Peak 1			Peak 2		
	A_q	ω_q (cm^{-1})	Γ_q (cm^{-1})	A_q	ω_q (cm^{-1})	Γ_q (cm^{-1})	A_q	ω_q (cm^{-1})	Γ_q (cm^{-1})
OTS	0.04	3300	20	1.81	3547	134.9	0.86	3647	107.9
BTSE	0.03	3300	20	1.76	3547	96.7	1.37	3665	115.6
TMOS	0.04	3300	20	1.27	3539	120	0.44	3665	120.0